NASA

Technical Memorandum 85021

X-RAY EMISSION FROM CLUSTERS OF GALAXIES

(NASA-TM-85021) X-RAY EMISSION FROM CLUSTERS OF GALAXIES (NASA) 31 p HC A03/MF A01 CSCL 03B
N83-33826
Unclas
G3/93 15011

R. F. Mushotzky

MAY 1983

National Aeronautics and
Space Administration

Goddard Space Flight Center
Greenbelt, Maryland 20771

X-RAY EMISSION FROM CLUSTERS OF GALAXIES*

R.F. Mushotzky

Laboratory for High Energy Astrophysics

NASA/Goddard Space Flight Center

Greenbelt, Maryland 20771 USA

ABSTRACT

We present a summary of X-ray spectral observations of 30 clusters of galaxies from HEAO-1. There exists strong correlations between X-ray luminosity, L_X, and temperature kT in the form $L_X \alpha T^{2.3}$. This result combined with the L_X vs central galaxy density relation and the virial theorem indicates that the core radius of the gas should be roughly independent of L_x or KT and that more luminous clusters have a greater fraction of their virial mass in gas. The poor correlation of KT and optical velocity dispersion, σ_v, seems to indicate that clusters have a variety of equations of state. There is poor agreement between X-ray imaging observations and optical and X-ray spectral measures of the polytropic index. Most clusters show Fe emission lines with a strong indication that they all have roughly 1/2 solar abundance. We discuss the evidence for cooling in the cores of several clusters based on spectral observations with the Einstein Solid State Spectrometer.

*To appear in Physica Scripta Proceedings of the Nice Workshop on Hot Astrophysical Plasmas held in Nice, France, November 8-10, 1982.

Clusters of galaxies are the largest ensemble of gravitationally bound matter in the universe. In the optical band clusters are characterized by the presence of tens of relatively large galaxies in a small, $V < 1/2$ Mpc^3, volume of space. It was one of the major discoveries of X-ray astronomy[1,2,3] that the space between the galaxies is occupied by a low density, $n < 10^{-3}$ particles/cm^3, hot, $T > 10^7$ ^oK, gas of roughly solar composition. In this paper we will review the detailed properties of this gas as revealed by past X-ray spectroscopic and photometric results and the correlations with the optical properties of the cluster.

I. LUMINOSITY FUNCTION

All sky X-ray surveys by the HEAO-1 satellite[4,5,6,7] have discovered X-ray emission from over 50 clusters of galaxies that are part of Abell's complete sample of optically discovered clusters of galaxies. That is, these clusters are rich enough (richness refers to the number of galaxies within a certain magnitude range of the brightest cluster galaxies, and within a per unit true distance from the cluster center on the sky) to be contained in Abell's catalog and are in that part of the sky that Abell sampled thoroughly. A uniform X-ray flux limit for detection of these clusters then allows one to construct a luminosity function.

At intrinsic luminosities greater than 2×10^{44} ergs/sec in the 2-10 keV band* the function is well fit by a power law of form $\zeta(L_x) = AL_{44}^{-2.0}$ ergs/sec Mpc^{-3} (10^{44} ergs/sec^{-1}) with $A \sim 2 \times 10^{-7}$. At lower luminosities the function must flatten so that the number density of "X-ray" clusters is not larger than that of optically selected clusters. Roughly speaking only 1/2 of all rich optical clusters have $L_x > 10^{43}$ ergs/sec in the 2-6 keV band[7].

There are several reasons why the luminosity function is not well

*I assume H_o = 50 Km/sec Mpc

determined at low luminosities, $L_X < 10^{43}$ ergs/sec. First of all there does not exist a complete optical catalog of poor clusters. Since these poor clusters tend to have low X-ray luminosities, any luminosity function based solely on Abell clusters will underestimate the space density of low luminosity clusters (but see ref. 8). Secondly at low luminosities ($L_X < 10^{43}$ erg/sec) the contribution of the hundreds of individual galaxies, whose intrinsic luminosities lie in the range 10^{39}-10^{42} ergs/sec, is an important contribution. Thus it becomes difficult with non-imaging experiments to separate the true "cluster" contribution from the superposition of individual galaxies. Finally there is a selection effect due to the band pass of the all sky survey experiments (Uhuru, Ariel 5, HEAO-1). These experiments were sensitive primarily in the 2-10 keV band. Thus clusters with kT < 2 keV were, typically, not detected by these instruments. Since, as we shall see, low temperature clusters have low luminosity this selection effect resulted in a dearth of low luminosity clusters.

II. X-RAY TEMPERATURES

There now exist good X-ray spectral measurements for ~ 40 clusters in the 2-40 keV band from experiments on OSO-8, Ariel-5 and HEAO-1. Because the HEAO-1 sample is the largest and also, in general, has the best statistics, we shall use the 30 clusters for which we have HEAO-1 temperatures as the basis for our discussion.

A. High Luminosity Clusters

Clusters whose luminosity in the 2-10 keV band is greater than ~ 5 x 10^{43} ergs/sec have a spectrum, in the 2-40 keV band, which is well described by an isothermal bremsstrahlung spectrum with kT $\gtrsim$ 2 keV. While several of these clusters have an additional cooler component due to a cooling flow in the cluster center, the contribution of this component to the 2-40 keV flux is low, usually less than 5%.

Because the all sky surveys were relatively insensitive to low energy, kT < 2 keV, objects the clusters with low temperatures are poorly represented in the sample. Therefore the cutoff in the apparent distribution of X-ray temperatures at kT ~ 2 keV is a selection effect. However, there appears to be a "maximum" observed X-ray temperature of kT $\gtrsim 10$ keV. This is not a selection effect but is probably related to the maximum depth of the cluster potential.

B. Low Luminosity Clusters

The small number of low luminosity clusters in the HEAO-1 sample almost all have complex spectra[9,10] which can be described as consisting of two components. The "softer" component can be well described as a low temperature, kT < 3 keV, thermal spectrum while the "hard" component can be fit by either a high, kT > 6 keV, temperature thermal component or a power law. In the best measured case, the Virgo cluster[11], the "hard" component is most likely a power law whose origin is in the active nucleus of M87. In the cases of the A1060, Centaurus, and A2147 clusters the nature of the "hard" component is not so clear. It is possible that in these clusters the "soft" component could be due to X-ray emission from massive individual galaxies (e.g. NGC 4696 in Centaurus) while the "harder" flux is due to the total cluster emission. Alternatively the "harder" flux could be due to inverse-Compton emission produced by relativistic electrons scattering off the 3° background radiation or to an active galaxy in or near the cluster. Several of the correlations and relationships discussed in the following sections give different indications as to the physical nature of the two different components. Only spatially resolved X-ray spectra of these clusters in the .5-10 keV range can settle this question. Spatial resolution of $\sim$ 1-2' is adequate for this task.

C. Correlations with X-Ray and Optical Properties

1. Temperature and Luminosity

Using OSO-8 and Ariel-5 data[12,13] it was determined that the X ray luminosities and X-ray temperatures were strongly correlated. However the relatively small size of the samples, the uncertainty in identifications and the relatively large errors in temperature for weak clusters made the form of the correlation uncertain.

When we use the HEAO-1 data (Figure 1) we find an extremely strong correlation of the form $L_X \propto T^{2.3 \pm .3}$ (where we have used the lower value of kT for the low luminosity clusters). If we use the higher value of kT for the low L_X clusters we find that the correlation breaks down at $L_X \sim 10^{44}$ erg/sec. We feel that this may indicate that it is the lower kT component which is more closely related to the total cluster contribution. This is likely to be the case because the emission integral for the low temperature component is larger, by a factor of 2-5, than that for the high temperature component. Alternatively, if the low kT component is due to individual galaxies, as may be true in Virgo, the correlation between L_X and kT may break down at low L_X. The two major exceptions to this trend, A2147 and 0335+096, are rather peculiar clusters. (It is interesting to note that the high temperature, $T > 1.5 \times 10^8$, component for A2147 does not appear to be on the regression line either but that the mean temperature, $kT \sim 7$ keV, does).

Since the X-ray luminosity, L_X, is proportional to $\langle n_e^2 V\rangle T^{1/2}$, where V is the volume of the cluster, n_e the density, T the temperature, this correlation means that the volume emission measure, $\langle n_e^2 V\rangle \sim T^{1.8}$. This result is somewhat flatter than the best fit OSO-8 and Ariel-5 determinations. Since the scatter in the effective emitting volume for X-ray clusters is small and apparently uncorrelated with luminosity[14,34] we can conclude, roughly, that the mean density of the gas $\langle n_e \rangle \propto T^{0.9}$, that is, hotter clusters are denser (a similar conclusion can be derived from the data in ref. 34). Since the mass in the gas is proportional to the central density (under the assumption of constant emitting volume) hotter, more luminous clusters must have more mass in gas than cooler clusters.

2. Temperature and Velocity Dispersion

From the OSO-8 and Ariel-5 surveys it seemed as if the X-ray temperature and optical velocity dispersions σ_v were well correlated but, again, the form of the correlation was poorly known. With the advent of larger data bases in the optical[15] and X-ray it is now possible to test the correlation in more detail, Figure 2. Here we see that, while in general clusters with higher velocity dispersions indeed have higher X-ray temperatures, there is a large scatter. The scatter is also of a rather peculiar form.

The intergalactic gas must conform to the gravitational potential in a rich cluster. If the gas and the galaxies are isothermal then the relationship between the galaxy density ρ_g and the gas density[19] n is $(n/n_0) = (\rho_g/\rho_0)^{\beta_1}$ where $\beta_1 = \mu m_H \frac{\sigma_v^2}{kT}$ with μ = mean molecular weight, m_H = mass of the hydrogen atom and n_0 and ρ_0 are the central values of the gas and galaxy density respectively. The ratio of galaxy to gas scale height is also β_1 in the isothermal limit. If one uses a King model for the cluster potential, the X-ray surface brightness is $S(r) = (1+r^2/a^2)^{(-3\beta_2 + 1/2)}$ where a is the core radius. It has been shown for quite a few clusters that[34], if a is adjustable, $\beta_2 \sim 1/2$ is a good fit to the X-ray surface brightness. In principle $\beta_1 = \beta_2$ if these models are a good description of the cluster. However inspection of Table I shows that only ~ .4 of the clusters for which we have both good X-ray temperatures and velocity distributions have β_1 compatible with 1/2. In fact this disagreement has been known for some time for the Perseus cluster[16]. In addition independent measures of the core radius[14] (where the authors have fixed $\beta = 1$) indicate that the X-ray core radius a_X is roughly 1.4 times the optical core radius, thus indicating that the gas and the galaxies do not have the same temperature. It is thus clear that isothermal models do not provide a good description of the totality of X-ray data.

Another simple alternative model is a polytropic model. In a polytropic model one can show[19] that the X-ray temperature, averaged over the entire cluster, should be approximately $T_X \sim 2.6\ (\sigma_V/1000\ \mathrm{km/s})^2$ keV for a polytropic index $\gamma = 1.05$ and $T_X \sim 10.3\ (\sigma_V/1000)^2$ keV for $\gamma = 5/3$ where again a King potential has been assumed. In Figure 2 we see that many clusters would have, in this model, $\gamma \lesssim 1.2$. However in a polytropic model one can show[31] that the X-ray surface brightness is roughly $S(r) \sim (1+\delta(r/a\ ^2)^{1/2-(1/\gamma-1)}$ where we have assumed that the gas is adiabatic, $\delta \sim .1$ and a_0 is the optical core radius. To fit the surface brightness data this model would require $\gamma \sim 5/3$ and $a_X \sim 3\ a_0$. As we have seen the indicated value of γ does not seem to fit the available spectral data either. It seems clear that a more complete approach[17] is necessary.

In an evolutionary scenario the gas relaxes before the galaxies since even in the core the relaxation time for the galaxies is close to the Hubble time. However the distribution of β_1 (Table I) does not seem to be obviously connected with the optical type of the cluster. Perhaps an X-ray imaging approach[18] might reveal if the values of β_2 are related to a parameter correlated with the degree of cluster evolution.

It is interesting that for the clusters that have two component spectra that the value of β_1, using the high temperature component is much more in line with the β_1 value of other clusters than when the low kT component is used (Table I). This suggests that the high energy component is thermal in nature and may be related to the depth of the cluster potential as seen by the galaxies. However this casts doubt on the physical reality of the L vs kT relation. It is clearly that spatially resolved spectral data are necessary to resolve this confusing problem.

Recent optical work[35] has indicated that many clusters show strong subclustering and that the velocity dispersion for the cluster as a whole may be seriously over estimated. Thus it is possible that the kT vs. velocity dispersion diagram may be dominated by this "non-virialization" of the galaxies. Of course X-ray images as well as optical galaxy counts may show which "clusters" are dominated by this effect. However, as Huchra and co-workers have shown, the Virgo cluster, previously assumed to be a single unit, has its previously determined velocity dispersion dominated by subclustering effects. This effect for Virgo would reduce the velocity dispersion by ~ a factor of 2 and thus put it much closer to the $\gamma \gtrsim 1.2$ line in Figure 2. Of course the values of β_1 are also affected. The sense of the effect would be to raise the measured value of β_1 over its true value. Our data suggests that, perhaps, in many clusters the galaxies are not virialized.

3. X-Ray Temperature, Luminosity and Central Galaxy Density

As has been shown previously with the OSO-8 data set[12,19], central galaxy density N_0 and the X-ray temperature T_X are extremely well correlated. In Figure 3 we show the result from the HEAO-1 sample. The best fit is of the form $T_X \propto N_0^{1.0\pm.2}$.

This fit can be combined with the temperature vs. luminosity correlation to predict a luminosity vs. N_0 correlation if we assume that the gas density and the galaxy density are linearly related, that is $n_e \propto N_0$. If this is true then the observed L_x vs. T relation, $L_x \propto \langle n_e^2 V\rangle T^{1/2} \propto T^{2.3}$, predicts that $L_x \propto N_0^{2.5\pm.5}$. As we see in Figure 4 the X-ray luminosity and central galaxy density are extremely well correlated. A best fit power law model gives $L_x \propto N_0^{3.5\pm.5}$, in agreement with the prediction.

It is also possible to use the observed L_x vs. N_0 relation to predict the correlation between L_x and T (again assuming that $n_e \propto N_0$). This assumption, of a linear relationship from cluster to cluster of gas and galaxy density, is not necessarily in conflict with the earlier discussion in which the gas and galaxy scale heights in a given cluster were shown to be not necessarily the same. However we cannot at present determine whether this linear relationship is the only one consistent with our data. In order to recover the measured relation one requires that the cluster's effective volume, V, be roughly independent of T. This does seem to be the case[14] when the core radii of clusters are directly determined, for example by the Einstein IPC. We are thus left with some quite interesting conclusions out of the L_x, N_0, T_x correlations.

First of all, it seems that the central galaxy density and the particle density are roughly linearly related. Secondly, it seems that the core radius (the effective volume) is roughly independent of the temperature, and finally that the X-ray temperature is correlated with the central density. In the context of a virial model the central density is defined by

$$\rho_0 = \frac{9\sigma^2}{4\pi G a_0^2}$$

where $3\sigma^2$ is the "effective" temperature and a_0 is the core radius. Thus $\rho_0 = \frac{3}{4\pi G} T/a_0^2$. We now think we know that $\rho_0 \propto T^{0.9}$ so one derives that $a_o \propto T^{.05}$ or that the core radius is independent of T. This agrees with the result of Bahcall[20] who finds no dependence of a_0 on cluster luminosity and with our T vs. N_0 correlation. Thus the fact that the core radius is roughly independent of luminosity or temperature is a "consequence" of the virial theorm and the observed X-ray temperature vs. density correlation. The correlation of L_x with T_x is also of physical interest. If the X-ray emitting gas is a faction δ of the virial mass, $M_{gas} = \delta M_{vir}$ then $\langle n_e^2 V\rangle \propto \delta^2 f\, T^2 a_0^2/V$, where $f = \langle n^2\rangle/\langle n\rangle^2 > 1$ is a central concentration factor for the gas[19]. Since we now know that $\langle n_e^2 V\rangle \propto T_x^{1.8}$, and since a_0 is independent of T_x, we surmise that $\delta^2 f$ is independent of T. This would argue for an approximately constant ratio of virial mass to gas mass to the ensemble of clusters.

III. X-RAY EMISSION LINES

The HEAO-1 detectors, sensitive in the 2-40 keV range, with a $1.5^0 \times 3^0$ field of view have sufficient spectral resolution to detect emission from the complex of Fe K shell lines from 6.4-8.5 keV. As shown in Figure 5 these lines due to Fe XXIV-XXVI are the strongest emission lines when the cluster temperature is > 2 keV. The Solid State Spectrometer (SSS) on the HEAO-2 (Einstein) Observatory is sensitive in the .5-4.0 keV band where one can see K shell lines from Mg, Si, S and Fe L shell lines. However, as Figure 5 shows, for kT > 3 keV these lines have low equivalent widths. In addition since the SSS had a 6' diameter beam it only sampled the central regions of the rich clusters. These combined characteristics make HEAO-1 relatively insensitive to any localized temperature variation (such as cooling) but the SSS very sensitive to these phenomena.

A. Fe K Lines

The ubiquity of Fe K line emission from clusters is established by the presence at greater than 3σ level of Fe emission in 26 out of 30 clusters for which we have good HEAO-1 A2 spectra. We see in Figure 6 that, for clusters which have a well defined simple component spectrum, the Fe abundance is remarkably uniform with <Fe> $\cong$ .55 solar for almost all the clusters. (This assumes <Fe/H> solar = 3.2×10^{-5}). This uniformity in Fe abundance is surprising in view of the different evolutionary and dynamical states of the clusters. This would argue that the iron in the intracluster gas does not, primarily, come from a process, such as stripping of galaxies within the last few 10^9 years, which depends on the evolutionary state of the cluster. This does not argue against models in which the Fe is produced in galaxies and stripped from them at relatively early times. Because both the ratio of virial mass to gas mass and the Fe abundance are roughly constant from cluster to cluster we feel that this argues for the creation of the intergalactic medium at quite early times. That is the properties of the intercluster medium are, relatively speaking, fixed and remain roughly constant with time if a clusters evolutionary state is a measure of that time.

The ratio of Fe Kα to Kβ emission seen in a few clusters[10] argues for rough isothermality. Increased sensitivity and spectral resolution is needed to use the Kα/Kβ ratio as a good temperature sensitive indicator.

B. Other Elements

Because of the weakness of the Mg, Si and S lines (see Figure 5) from gas at kT > 2 keV the limits to the abundances of these elements as determined by the Einstein SSS are relatively poor. For several clusters (A496, A2199, A576, 0335+096, A426) it is possible to show that the Si and S abundances are between .3 and 3 times solar. For several other clusters (A1795, A2029, A85, etc) one can only show that the inclusion of lines due to metals (S, Si, Fe, Mg) significantly improves the fit. Thus, with a fair degree of confidence one can state that most clusters have roughly solar abundances of S, Si and Mg as well as Fe. Larger collecting areas and better spectral resolution are needed to improve on this data.

IV. COOLING CORES IN CLUSTERS

The cooling of gas in the centers of rich clusters in a time less than a Hubble time was predicted to occur by several workers[21,22,23]. The effects of this cooling on both the low energy X-ray spectra and the X-ray surface brightness profile has been detected[24,25,26] from a few rich luminous clusters.

The signature of cooling is the appearance of lines due to Fe, Si and S which originate from ions that are only present, in equilibrium, at temperatures less than the temperature of the bulk of the X-ray emitting gas in a rich cluster. As shown in Figure 5 the signature could, in principle, be clear since the helium like lines of Si and S have their peak emissivity at $kT < 2$ keV. The Fe XVII-XXII blends also peak at $kT < 2$ keV. The problem is that while the equivalent width (EW) due to the low kT component is large for these lines, their measurable EW is reduced by the <u>hot</u> component of the gas. Thus the <u>signal</u> due to the cooler gas is diluted by the hot, non-cooling cluster gas. Fortunately the line ratios of Si XIII-XV and S XIV-XVI are not affected by the dilution. In addition, the EW of Fe L lines is so large that they stand out strongly above the diluting continuum in several sources. The effect of dilution can be lessened by a smaller beam size and the measurement of temperature sensitive line ratios could be improved by better energy resolution.

Since the gas is in rough pressure equilibrium the effect of cooling on the X-ray image is to increase the surface brightness at small physical distances from the core to levels substantially above what a hydrostatic polytropic model would predict[26]. The detection of this increase in surface brightness typically requires HRI observations on the Einstein Observatory, and is sometimes difficult to distinguish from the presence of a point source at the cluster center.

The combination of X-ray surface brightness measurements and X-ray spectroscopy is a powerful tool to study cooling. Cooling is expected to become important when the cooling time is less than the Hubble time. Since at $kT > 4$ keV most of the cooling is due to thermal bremsstrahlung one can parameterize a cooling radius as $R \cong (3.3\, n_{-2}^{2/3} - 1)^{1/2}$ where we have normalized the clusters density by $n_{-2} = 10^{-2}$ cm^{-3}. R is the distance in core radii, a, at which the cooling time equals the Hubble time. Thus only at distances less than .4 typical core radius (~ .1 Mpc or ~ 2' at 200 Mpc) should cooling be important.

A major question that has arisen[18] is whether the gas is really cooling. That is, is it possible for some heat source, for example relativistic particles or photons from an active nucleus, to supply enough heat to keep the gas from cooling? In the case of M87 one has ~ 10 M_0/yr of thermally unstable, "cooling" gas[32,33], therefore an energy input of roughly $3\,(\frac{kT}{\mu m_H})\,\dot{M} \sim 3 \times 10^{42}$ erg/sec is required to keep it hot. However in the core of Perseus or A496 an energy input 30 times larger or ~ 1×10^{44} ergs/sec, in heat, is required to prevent cooling. Of course the situation has to be well balanced; if the heat input drops, cooling will recommence while if the heat input increases, there will be a wind blown out of the cluster.

If the supernovae rate in the cooling gas (1 per 10^{13} M_0/yr) is the same as in our galaxy this is not a sufficient energy source to heat the gas. But if the rate per unit mass were 10^3 times higher the self-heating from supernovae would stop the cooling flow.

B. Results

We have seen evidence for cooling in ~ 7 clusters (Table II) with the SSS. For at least two of these, A496 and A426 (Perseus)[25,26] there exist surface brightness maps that provide corroborative evidence for a cooling flow. We notice that there does not exist a wide range of the ratio $\dot{M}/L_x$, a measure of the ratio of the amount of cooling gas to the total cluster mass. The highest ratio is for M87, but this depends rather strongly on what one calls the luminosity of M87[27]. If we use the luminosity of M87 out to 100' then this ratio is $(1-5)\times10^{17}$, consistent with the other clusters. With that exception the ratio varies from $(2-10)\times10^{17}$, a fairly small bound.

All the clusters for which cooling has been observed are centrally condensed clusters. A subset of these clusters have been observed by various workers[28,29,30] looking for signs in the optical band for the cooling flow. The gas that cools down to ~ 10^4 K should produce roughly 1 Hα photon per cooling ion. Thus a sign of cooling gas in the cluster would be the presence of Hα remission filaments located in the cluster centers. These features have now been seen in quite a few clusters and its presence seems to confirm the cooling hypothesis.

CONCLUSION

X-ray spectral observations of clusters of galaxies have determined the temperature and abundance of Fe in roughly 25 clusters. In addition strong evidence for cooling in the centers of ~ 7 clusters has been found. There exists strong correlations between the X-ray luminosity and temperature, and the optical galaxy density. The lack of good detailed correlation between the optical velocity dispersion and the X-ray temperature has to be explained by models of cluster formation and evolution, and detailed modeling of the "equation of state" of the cluster is required. Alternatively this lack of correlation may be due to the lack of virialization of the galaxies as evidenced by velocity substructure.

There is much work yet to be done. We need spatially resolved X-ray spectra to determine the temperature gradient. This is the major undetermined parameter for cluster models. Such data will also show if abundance gradients exist. Higher signal to noise and greater collecting area combined with moderate resolution ($\Delta E/E \lesssim .1$) are needed to see if the abundance of Fe is a function of redshift (Z) and to look for evolutionary changes in Fe abundance. Similar instrumentation will enable temperatures and abundances to be determined for the ~ 200 X-ray emitting clusters detected by the Einstein Observatory. (Most of these clusters should have low kT's and thus strong line emission). Higher energy resolution spectra with good signal to noise and moderate spatial resolution are necessary to tackle the problem of cooling cores. If enough lines are measured then a semiunique model of the cooling flow can be determined. The instruments on X-80 are well suited to these problems and should reap a rich harvest of results.

ACKNOWLEDGMENTS

I thank S. Holt, R. White, E. Hu, G. Reichert, A. Fabian and C. Sarazin for informative and interesting conversations, and E. Boldt and P. Serlemitsos for making this project possible. I thank the organizers of the Nice Workshop, particularly H. Schnopper and L. Koch for the opportunity to attend this exciting meeting.

REFERENCES

1) Forman, W., Kellogg, E., Gursky, H., Tananbaum, H. and Giacconi, R. 1972, Ap. J. 178, 309.

2) Mitchell, R.J., Culhane, J.L., Davison, P.J.W. and Ives, J.C. 1976, M.N.R.A.S. 175, 29p.

3) Serlemitsos, P.J., Smith, B.W., Boldt, E.A., Holt, S.S. and Swank, J.H. 1977, Ap. J. (Letters) 211, L63.

4) McKee, J.D., Mushotzky, R.F., Boldt, E.A., Holt, S.S., Marshall, F.E., Pravdo, S.H. and Serlemitsos, P.J. 1980, Ap. J. 242, 843.

5) Piccinotti, G., Mushotzky, R.F., Boldt, E.A., Holt, S.S., Marshall, F.E., Serlemitsos, P.J. and Shafer, R.A. 1982, Ap. J. 253, 485.

6) Ulmer, M.P. et al. 1980, Ap. J. 243, 681.

7) Johnson, M.W., Cruddace, R.G., Ulmer, M.P., Kowalski, M.P. and Wood, K.S. 1983, Ap. J.,

8) Bahcall, N.A. 1979, Ap. J. (Letters) 232, L83.

9) Pravdo, S.H., Boldt, E.A., Marshall, F.E., McKee, J., Mushotzky, R.F., Smith, B.W. and Reichert, G. 1979, Ap. J. 234, 1.

10) Mitchell, R.S. and Mushotzky, R.F. 1980, Ap. J. 236, 730.

11) Lea, S.M., Reichert, G., Mushotzky, R.F., Baity, W.A., Gruber, D.E., Rothschild, R., and Primini, F.A. 1981, Ap. J. 246, 369.

12) Mushotzky, R.F., Serlemitsos, P.J., Smith, B.W., Boldt, E.A., and Holt, S.S. 1978, Ap. J. 225, 21.

13) Mitchell, R.J., Dickens, R.J., Bell-Burnell, S.J. and Culhane, J.L. 1979, M.N.R.A.S. 188,

14) Abramopoulous, F. and Ku, W.H-M. 1983, Ap. J., in press.

15) Quintana, J and Melnick, G. 1982, AJ 87, 972.

16) Branduardi-Raymont, G., Fabricant, D., Feigelson, E., Gorenstein, P., Grindlay, J., Soltan, A. and Zamorani, G. 1981, Ap. J. 248, 55.

17) Cavaliere, A., these proceedings.

18) Forman, W. and Jones, C. 1982, Annual Review of Astronomy and Astrophysics, Vol XX, pg. 49.

19) Smith, B.W., Mushotzky, R.F. and Serlemitsos, P.J. 1979, Ap. J. 227, 37.

20) Bahcall, N. 1974, Ap. J. 187, 439.

21) Fabian, A. and Nulsen, P.E.J. 1977, M.N.R.A.S. 180, 479.

22) Cowie, L.L. and Binney, J. 1977, Ap. J. 215, 723.

23) Mathews, W.G. and Bregman, S.N. 1978, Ap. J. 224, 308.

24) Mushotzky, R.F., Holt, S.S., Smith, B.W., Boldt, E.A. and Serlemitsos, P.J. 1981, Ap. J. (Letters) 244, L47.

25) Fabian, A.C., Hu, E.M., Cowie, L.L. and Grindlay, J. 1981, Ap. J. 248, 47.

26) Nulsen, P.E.J., Stewart, G.G., Fabian, A.C., Mushotzky, R.F., Holt, S.S., Ku, W.H-M. and Malin, P.F. 1982, M.N.R.A.S. 199, 1089.

27) Fabricant, D. and Gorenstein, D. 1983, CFA preprint 1741.

28) Heckman, T. 1981, Ap. J. 250, L59.

29) Fabian, A.C., Ku, W.H-M., Malin, D.F., Mushotzky, R.F., Nulsen, P.E.J., Stewart, G.C. 1981, M.N.R.A.S. 196, 35.

30) Cowie, L.L., Hu, E., Jekins, E.B. and York, D.G. 1983, Ap. J., in press.

31) Sarazin, C. 1981, private communication.

32) Canizares, C.R., Clark, G., Jernigan, G. and Markert, T. 1982, Ap J. 262, 33.

33) Lea, S., Mushotzky, R.F. and Holt, S.S. 1982, Ap. J. 262, 24.

34) Jones, C. and Forman, W. 1983, Ap. J., submitted.

35) Huchra, J. 1983, invited talk at Baltimore A.P.S. meeting.

FIGURE CAPTIONS

Figure 1 - The mean X-ray temperature for several clusters vs their 2-10 keV luminosity.

Figure 2a - X-Ray temperature vs optical velocity dispersion. Typical error bars are shown. Lines of constant polytropic index are drawn. An open circle indicates a cD type cluster.

Figure 2b - Optical velocity dispersion vs X-ray temperature. Lines of constant slope $kT \alpha v^2$ are indicated.

Figure 3 - X-ray temperature kT vs central galaxy density N_0. Best fit linear regression lines are indicated.

Figure 4 - X-ray luminosity (2-10 keV) vs central galaxy density.

Figure 5 - Theoretical line equivalent widths for solar abundance gases in equilibrium from Raymond and Smith (1977). The numbers on the line are the mean energy of the line complexes as seen by a moderate resolution detector.

Figure 6 - The abundance of Fe determined for 17 clusters vs their X-ray luminosity.

TABLE I

X-Ray Temperatures, Velocity, Dispersions and β Values for Clusters

NAME	kT^+	σ_V^{++}	β_1
A119	5.2 ± 1.0	778^{+160}_{-100}	.73 ± .28
AWM7	3.95 ± .50	830^{+161}_{-104}	1.10 ± .37
A401	6.55 ± 1.0	1289^{+352}_{-195}	$1.60^{+.89}_{-.53}$
0316-44	$7.0^{+1.5}_{-1.0}$	788^{+174}_{-108}	.55 ± .22
A426	6.4 ± .40	1282^{+95}_{-78}	1.60 ± .24
0340-53	$5.5^{+.70}_{-1.4}$	1006^{+222}_{-135}	1.16 ± .47
A576	$3.5^{+3.0}_{-1.0}$	1211^{+254}_{-158}	$2.64^{+2.47}_{-1.00}$
Ser 40/6	8.2 ± .50	1517^{+252}_{-167}	1.77 ± .49
A754	8.2 ± .80	1196^{+230}_{-147}	1.10 ± .36
	6.5 ± 1.0*		1.39 ± .48
A1060	2.0 ± .7	777^{+159}_{-99}	1.90 ± .90
	6**		.63
Virgo	3.5, 2.2 ± .2	705 ± 100	.9, 1.4 ± .42
	> 8**		< .4
Centaurus	2.3 ± .5	870^{+88}_{-70}	2.07 ± .57
	6**		.80
Coma	8.0 ± 4	905^{+49}_{-43}	.64 ± .08
A1795	$6.5^{+.50}_{-.30}$	778^{+226}_{-124}	$.59^{+.34}_{-.18}$
	$5.4^{+.60}_{-.60}$ *		$.71^{+.41}_{-.23}$
A2029	6.2 ± 1.5	1424^{+178}_{-128}	2.06 ± .65
A2142	8.4 ± 1.60	1241 ± 358	1.16 ± .69

A2147	1.7 ± .9	1132^{+188}_{-132}	4.75 ± .55
	8**		1.00
A2199	3.6 ± .60	784^{+100}_{-75}	1.07 ± .28
	$3.9^{+.40}_{-1.2}$*		.99 ± .31
A2319	$8.9^{+2.1}_{-2.1}$	1580^{+249}_{-170}	1.76 ± .63
2009-569	$6.2^{+.70}_{-.75}$	1470^{+291}_{-183}	$2.20^{+.89}_{-.60}$
A2589	$3.9^{+.80}_{-1.20}$	602^{+176}_{-98}	.58 ± .36

* Indicates temperature from argon HEAO-1 A2 detector, errors are 90% confidence.

** Indicates higher temperature of a 2 component spectrum

+ Data from HEAO-1 A2 xenon detector, errors are 90% confidence

++ Optical velocity dispersions from ref. 15.

TABLE II

Cooling Rates in Cluster Cores

Cluster	$\dot{M}/L_x \cdot 10^{-17}$	$\dot{M}$ (M_o/yr)	L_x^{2-10}
A85	< 3.4	< 430	8×10^{44}
A401	< 2.3	< 670	18 "
A426	1.4	~ 270	12 "
A478	< 1.9	< 730	24 "
A496	4.8	200	2.6 "
A1795	3.2	560	11 "
A2029	1.0	280	17 "
A2142	< 1.3	< 540	27 "
A2199	1.2	~ 60	3.2 "
M87	13	~ 2-10	~ 5×10^{42}
	.2-2		~ 5×10^{43}
0335+096	4.2	~20	~ 3×10^{44}

$\dot{M}/L_X$ in units of gm/erg-sec

Data are from Einstein SSS results.

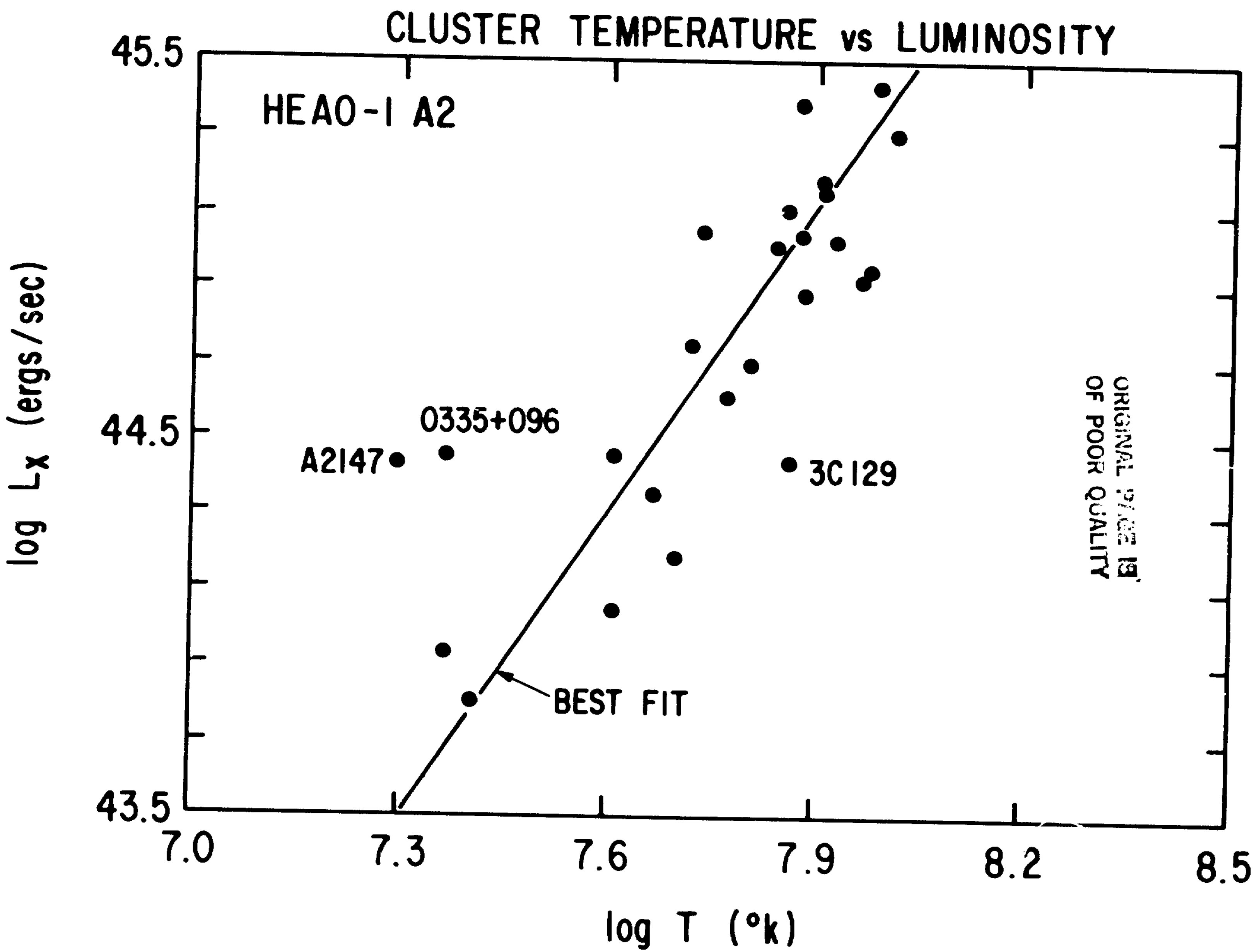
CLUSTER TEMPERATURE vs LUMINOSITY
HEAO-I A2
45.5
44.5
43.5
log Lx (ergs/sec)
A2147
0335+096
3C129
BEST FIT
7.0
7.3
7.6
7.9
8.2
8.5
log T (°k)

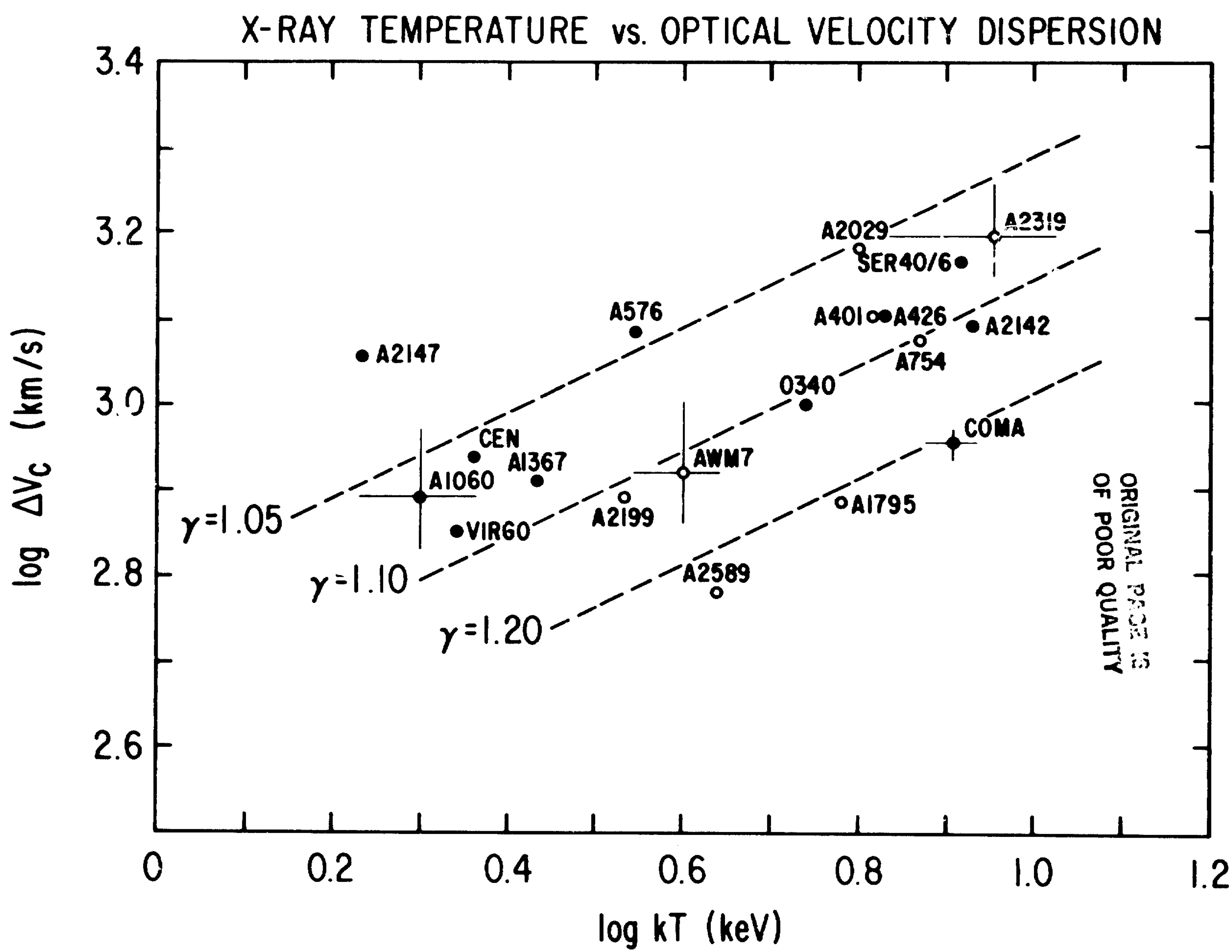
X-RAY TEMPERATURE vs. OPTICAL VELOCITY DISPERSION
log ΔVc (km/s)
log kT (keV)
3.4
3.2
3.0
2.8
2.6
0
0.2
0.4
0.6
0.8
1.0
1.2
A2147
A576
CEN
A1367
A1060
VIRGO
A2199
AWM7
A2589
0340
A2029
A2319
SER40/6
A401
A426
A2142
A754
COMA
A1795
γ=1.05
γ=1.10
γ=1.20
ORIGINAL PAGE IS
OF POOR QUALITY

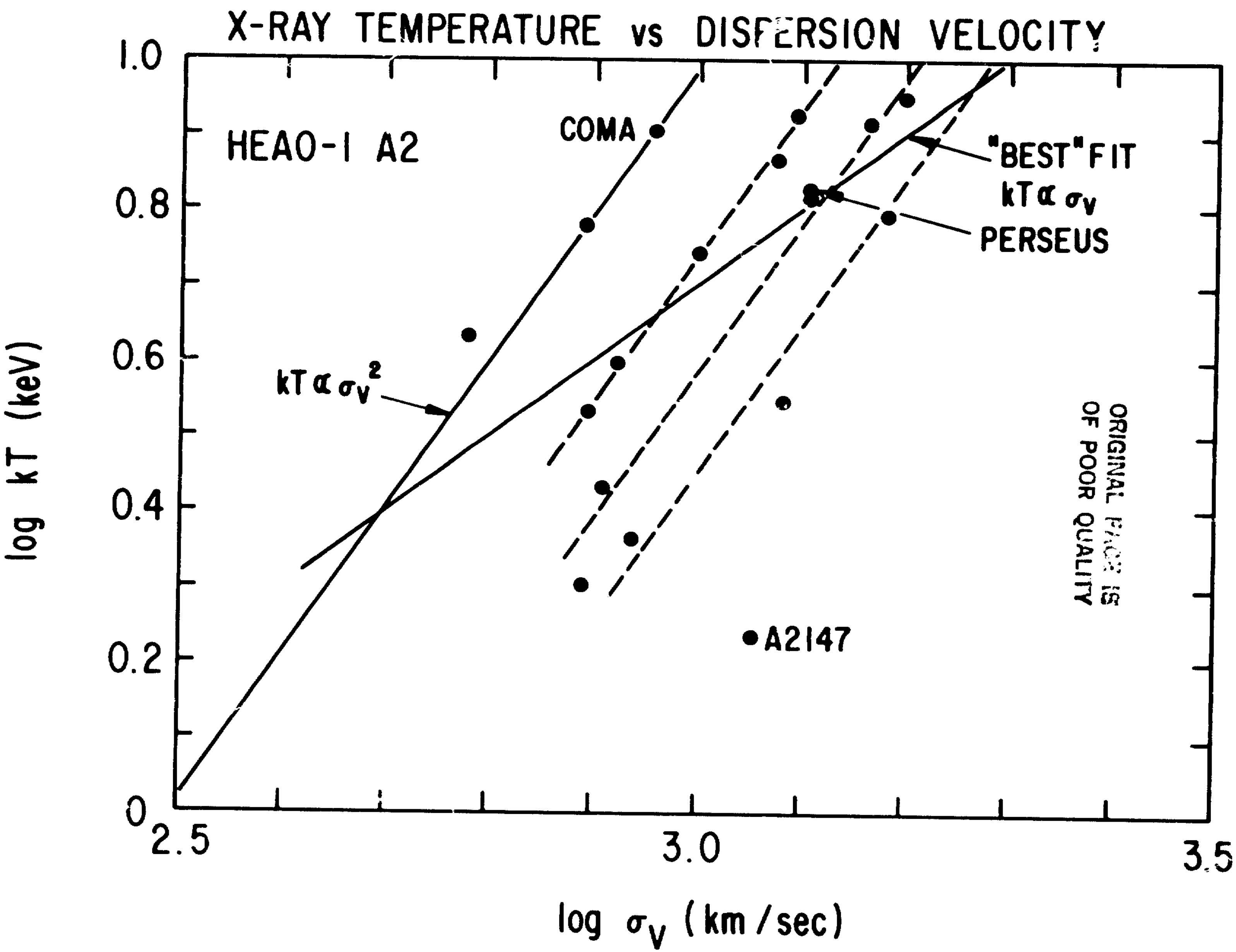
X-RAY TEMPERATURE vs DISPERSION VELOCITY
HEAO-I A2
COMA
"BEST" FIT
kT α σv
PERSEUS
kT α σv²
A2147
log kT (keV)
log σv (km/sec)
1.0
0.8
0.6
0.4
0.2
0
2.5
3.0
3.5

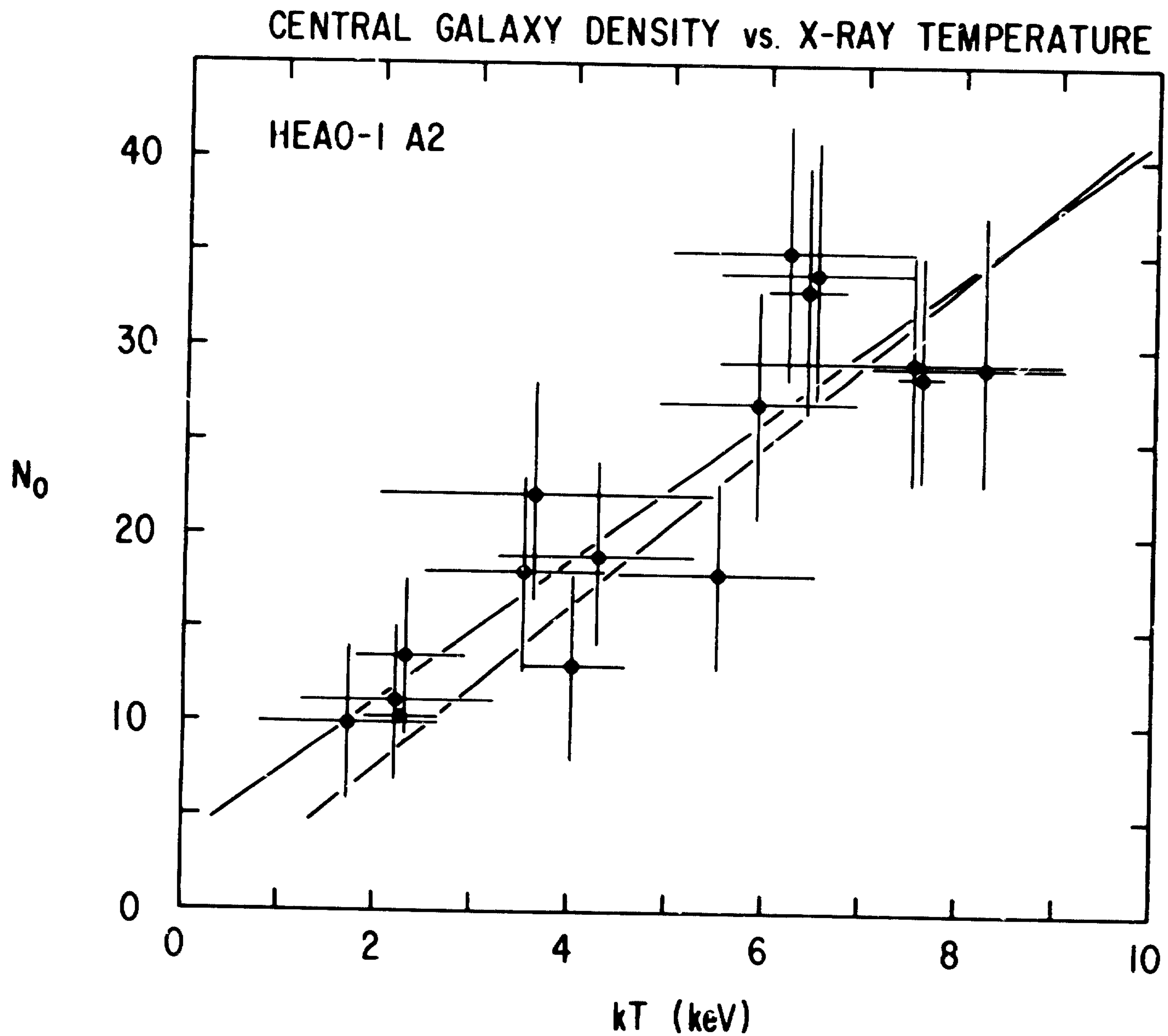
CENTRAL GALAXY DENSITY vs. X-RAY TEMPERATURE
HEAO-1 A2
N_0
0
10
20
30
40
0
2
4
6
8
10
kT (keV)

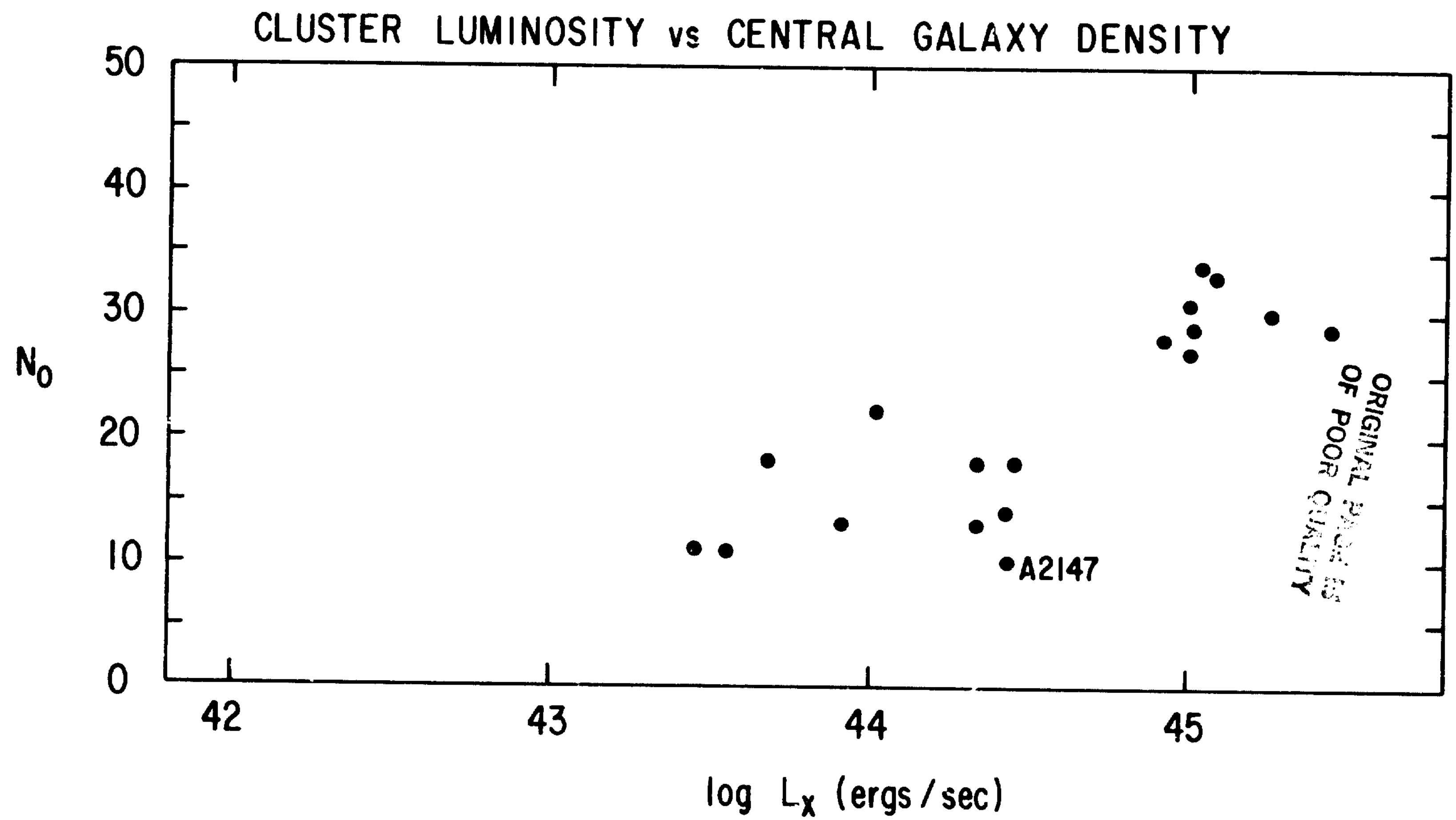
CLUSTER LUMINOSITY vs CENTRAL GALAXY DENSITY
N_0
50
40
30
20
10
0
42
43
44
45
log L_X (ergs / sec)
A2147

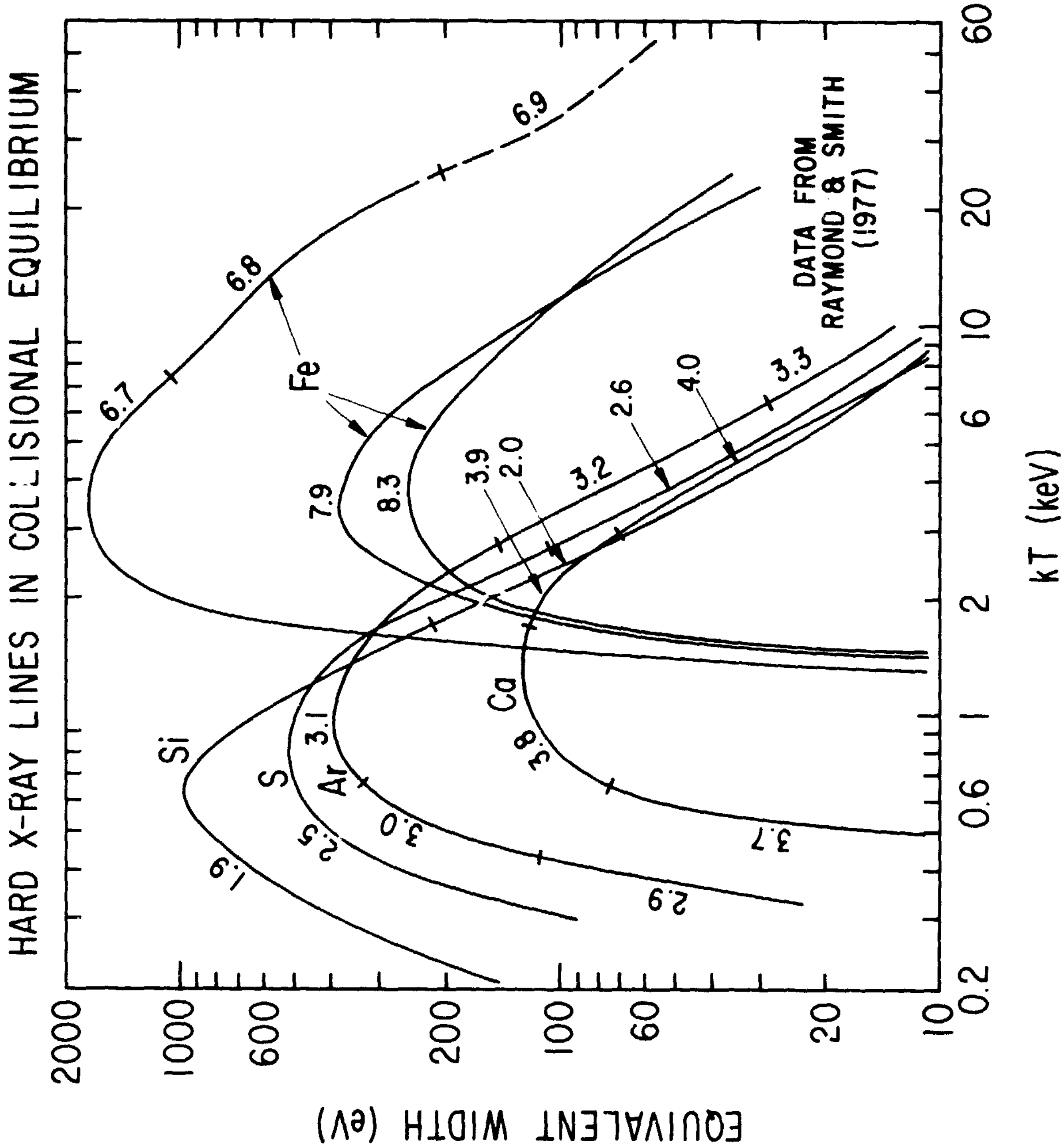
HARD X-RAY LINES IN COLLISIONAL EQUILIBRIUM
EQUIVALENT WIDTH (eV)
kT (keV)
2000
1000
600
200
100
60
20
10
0.2
0.6
1
2
6
10
20
60
Fe
Si
S
Ar
Ca
6.7
6.8
6.9
7.9
8.3
3.9
2.0
3.2
2.6
4.0
3.3
3.1
3.8
1.9
2.5
3.0
2.9
3.7
DATA FROM
RAYMOND & SMITH
(1977)

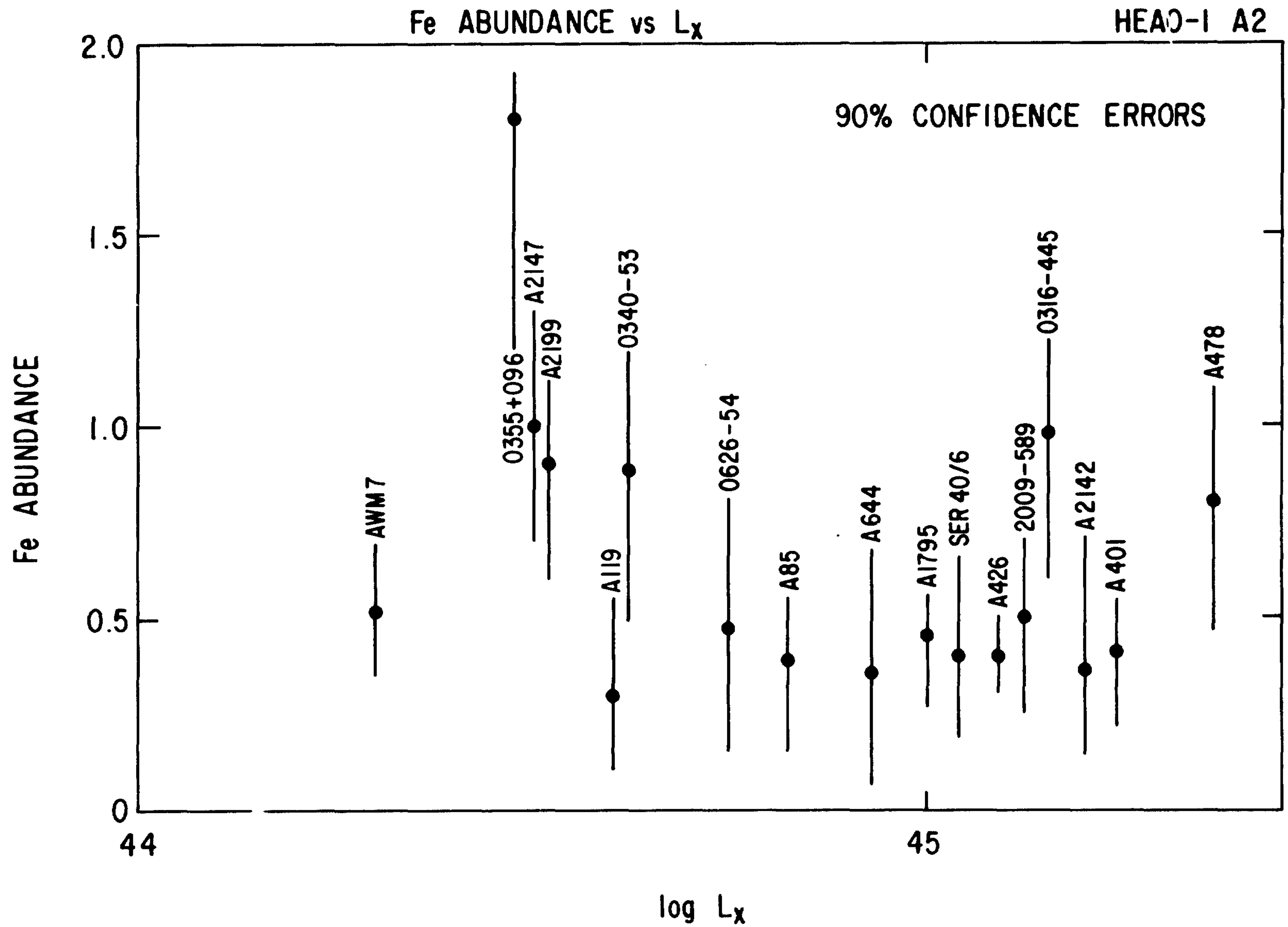
Fe ABUNDANCE vs L_x
HEAO-1 A2
90% CONFIDENCE ERRORS
Fe ABUNDANCE
2.0
1.5
1.0
0.5
0
44
45
log L_x
AWM7
0355+096
A2147
A2199
A119
0340-53
0626-54
A85
A644
A1795
SER 40/6
A426
2009-589
0316-445
A2142
A401
A478